

Signatures of MSSM charged Higgs bosons via chargino–neutralino decay channels at the LHC

M. Bisset^{1,a}, M. Guchait^{2,b}, S. Moretti^{3,c,d}

¹ Department of Physics, Tsinghua University, 100084 Beijing, P.R. China

² DESY Theorie, Notkestrasse 85, 22603 Hamburg, Germany

³ Particle Physics Department, Rutherford Appleton Laboratory, Chilton, Didcot, Oxon OX11 0QX, UK

Received: 21 October 2000 / Published online: 23 February 2001 – © Springer-Verlag 2001

Abstract. We assess the potential of detecting a charged Higgs boson of the MSSM at the LHC via its decays into a chargino and a neutralino. We focus our attention on the region of parameter space with $m_{H^\pm} > m_t$ and $3 \lesssim \tan\beta \lesssim 10$, where identification of the H^\pm via other decay modes has proven to be ineffective. Searching for means to plug this hole, we simulate the decays $H^\pm \rightarrow \tilde{\chi}_1^\pm \tilde{\chi}_1^0$ and $H^\pm \rightarrow \tilde{\chi}_1^\pm \tilde{\chi}_2^0, \tilde{\chi}_1^\pm \tilde{\chi}_3^0$ – the former can yield a single hard lepton (from the chargino decay) while the latter can yield three leptons (from the chargino and neutralino decays). Coupled with the dominant top quark + charged Higgs boson production mode, the resulting signature is one or three hard, isolated leptons, substantial missing transverse momentum and a reconstructed (via a 3-jet invariant mass) top quark. The single lepton channel is swamped by background processes; however, with suitable cuts, a tripleton signal emerges. While such a signal suffers from a low number of surviving events (after cuts) and is dependent on several MSSM input parameters (notably M_2 , μ , and slepton masses), it does fill at least some of the void left by previous investigations.

A pair of spin-0 charged Higgs bosons, H^\pm , arises in any two Higgs doublet model (2HDM) alongside a trio of neutral Higgs bosons – the $CP = +1$ “light” h and “heavy” H (with $m_h < m_H$) and the $CP = -1$ “pseudoscalar” A . The charged Higgs bosons have been at the focal point of extensive studies since they have no standard model (SM) counterpart, and thus could provide irrefutably clear evidence of an extended Higgs sector and new physics beyond the SM. On the other hand, it may be difficult to either distinguish one type of neutral 2HDM Higgs boson from the SM Higgs boson or observe more than one of the neutral species [1–4]. Embedding the 2HDM inside the attractive theoretical framework of supersymmetry (SUSY) yields (together with additional assumptions about minimal field content and minimal number of new couplings) the minimal supersymmetric standard model (MSSM). In the MSSM, at tree level, the masses of all Higgs bosons, along with their couplings to the SM fermions and gauge bosons, can be parametrized in terms of only two unknown input parameters, generally taken as the mass of one of the Higgs bosons (typically either m_A or m_{H^\pm}) and the ratio of the vacuum expectation values (VEV’s) of the up-type and down-type Higgs doublets (denoted by $\tan\beta$) [5].

As is well known [6], these tree level relations can receive substantial radiative corrections, most importantly enabling $m_h > M_Z$ (making the upper limit on m_h in the MSSM ~ 135 GeV [7]). However, the tree level relation between the masses of the charged Higgs bosons and A , $m_{H^\pm}^2 = m_A^2 + M_{W^\pm}^2$, is almost invariably quite insensitive to such corrections [8]. Properly taking into account the corrections to the light Higgs boson mass, m_{H^\pm} may still be related to m_h , and an indirect lower bound of ~ 140 GeV [9] for $\tan\beta \simeq 3$ –4 can be placed on the former due to the thus far null search for a Higgs boson at LEP2. This bound grows rapidly stronger as $\tan\beta$ is decreased while tapering very gradually as $\tan\beta$ is increased (staying in the 110–125 GeV interval for $\tan\beta \gtrsim 5$). There are also other processes where charged Higgs bosons (or A^0 , to whose mass that of the H^\pm is closely tied) enter as virtual particles at the one-loop level. These include neutral meson mixing ($K^0 \bar{K}^0$, $D^0 \bar{D}^0$, or $B^0 \bar{B}^0$) [10,11], $Z^0 \rightarrow b\bar{b}$ (R_b) [11,12], and $b \rightarrow s\gamma$ decays [10–13]. The $b \rightarrow s\gamma$ decays are generally thought to be the most constraining [12]. Here restrictions on m_{H^\pm} are linked to a number of MSSM variables, notably including the masses of the lighter chargino and the stops. We reserve further comment on this somewhat complex issue until after we present our results.

More direct limits on charged Higgs bosons come from hadron collider searches¹ for lepton non-universality (ex-

^a e-mail: bisset@mail.tsinghua.edu.cn

^b e-mail: guchait@mail.desy.de

^c e-mail: stefano.moretti@cern.ch

^d Current address: Theory Division, CERN, 1211 Geneva 23, Switzerland

¹ There are also direct searches for charged Higgs boson pair production at LEP2; however, bounds obtained in this way are

cess taus) in top quark decays resulting from $t \rightarrow bH^+$ followed by $H^+ \rightarrow \tau^+\nu_\tau$ [16] and the charge-conjugate reactions² (excessive numbers of charmed final states in top decays resulting from $H^+ \rightarrow \bar{s}c$ may also be of use, as well as $H^+ \rightarrow W^+b\bar{b}$ [17] for $\tan\beta \simeq 1$). At the soon to commence Run II of the upgraded Fermilab Tevatron, such channels will allow experimenters to scan the MSSM parameter space for *large and small values of* $\tan\beta$ roughly up to the kinematical limit of the $t \rightarrow bH^+$ decay, $m_t - m_b$ [18]. The reason for the $\tan\beta$ dependence stems from the couplings between a charged Higgs boson and top and bottom quarks, given by³

$$\sim \frac{g^2}{2M_{W^\pm}^2} H^+ (m_t \cot\beta \bar{t}b_L + m_b \tan\beta \bar{t}b_R). \quad (1)$$

The square of this, which has a minimum at $\tan\beta \simeq 6-7$, is proportional to the strength of either the $g\bar{b} \rightarrow \bar{t}H^+$ cross-section or the $t \rightarrow bH^+$ decay width. In the intermediate $\tan\beta$ region around this minimum, a Tevatron search for charged Higgs boson pair production, $q\bar{q} \rightarrow H^+H^-$, which mainly proceeds utilizing only gauge couplings, could be feasible [19] if the charged Higgs bosons are light enough – certainly $m_{H^\pm} \lesssim m_t$. As the mass of the charged Higgs boson grows larger than m_t , simple phase space suppression will severely handicap pair production.

Thus the likely legacy bequeathed to the Large Hadron Collider (LHC) will be the pursuit of a *heavy* charged Higgs boson (with $m_{H^\pm} \gtrsim m_t$). At the LHC, the dominant production mechanism for heavy H^\pm scalars is via the $2 \rightarrow 2$ reaction $g\bar{b} \rightarrow \bar{t}H^-$ [21] and the $2 \rightarrow 3$ reaction $gq \rightarrow t\bar{b}H^-$ [22]. Alternative production modes⁴ are charged Higgs pair production, $gg, q\bar{q} \rightarrow H^+H^-$ [24], and associated production, $gg, q\bar{q} \rightarrow W^\pm H^\mp$ [25]. The former suffers from a lack of phase space for $m_{H^\pm} > m_t$ and low quark parton luminosities ($q\bar{q}$) in the LHC protons or heavy propagator loop suppression (gg). The latter suffers from a huge irreducible background induced by either $t\bar{t}$ and/or W^+W^- production and decay, depending upon whether the charged Higgs boson decays via $b\bar{t}, W^-h$ or $\tau^-\bar{\nu}_\tau$ states [26]. For the preferred production mechanism, henceforth to be collectively referred to as the top- H^\pm production mode, the $\tan\beta$ dependence follows from the square of (1), again making high and low $\tan\beta$ values more accessible. The connection between the $2 \rightarrow 2$ and the $2 \rightarrow 3$ reactions has been discussed numerous times before [27, 28]; the former is obtained from the latter if one of the gluons splits into a $b\bar{b}$ pair, with one bottom quark, i.e., b - or \bar{b} -quark) then interacting with the remaining gluon while the other is assumed to act as a spectator. The

relatively low, $m_{H^\pm} > 77.5-78.6$ GeV [14]. At a future 500 GeV e^+e^- linear collider, this could increase to a potentially competitive ~ 210 GeV [15]

² Hereafter, inclusion of charged-conjugate processes may be assumed unless explicitly excluded

³ Analogous formulæ hold for the other two SM fermion generations

⁴ The $bq \rightarrow bH^\pm q'$ mode of [23] can only be relevant for very high values of $\tan\beta$

appropriate procedure [28, 29] for estimating the inclusive Higgs production cross-section is to combine the $2 \rightarrow 3$ subprocess with the $2 \rightarrow 2$ subprocess through the subtraction of a common logarithmic term $\sim \alpha_s \log(Q^2/m_b^2)$.

However, utilizing the $2 \rightarrow 2$ simulation for the kinematical event selection (and thereby tacitly assuming that the final state bottom quark manifest in the $2 \rightarrow 3$ formulation is soft and thus untaggable) could lead to erroneous event-shape parameter distributions (transverse momentum, opening angles between jets, etc.) due to the possible presence of the extra, neglected b -jet. Therefore, here we simulate both subprocesses: $2 \rightarrow 2$ simulations are employed solely to normalize the cross-sections, making use of this subtraction procedure, while $2 \rightarrow 3$ simulations are used to implement our selection and acceptance cuts with the b -jet resulting from the bottom quark produced in the $2 \rightarrow 3$ reaction subject to the same acceptance, resolution and isolation criteria as any other jet in that event.

Several decay modes for heavy H^\pm states (for branching ratio studies, see [30]), have been analyzed assuming the above top- H^\pm production mechanism, including: $H^- \rightarrow b\bar{t}$ [27, 31], *generally expected* to be the dominant decay mode; $H^- \rightarrow s\bar{c}$ (in the ATLAS study of [31]); $H^- \rightarrow W^-h$ [32]; and $H^- \rightarrow \tau^-\bar{\nu}_\tau$ [33]. All these decay modes (that will hereafter be termed “SM” decays) were simulated (including parton shower, hadronization and detector effects) in either the ATLAS simulations of [31–33] and/or in [20], with the latter concluding that H^\pm scalars with masses up to ~ 400 GeV can be discovered by the LHC, *but only if* $\tan\beta \lesssim 3$ (which is in the neighborhood of the indirect limit from LEP2) *or* $\tan\beta \gtrsim 25$. The ATLAS studies roughly concur, adding that the $H^- \rightarrow \tau^-\bar{\nu}_\tau$ channel can push the high $\tan\beta$ reach down below 20 for $m_{H^\pm} \lesssim 400$ GeV, with a minimum at $\tan\beta \approx 10$ when m_{H^\pm} is close to m_t .

The purpose of this paper is to assess the prospects for utilizing the thus far neglected SUSY decay channels of the MSSM charged Higgs bosons to probe regions of the parameter space inaccessible at the LHC via the SM decay modes. The charged Higgs boson can in fact decay predominantly via these SUSY modes, as illustrated in Fig. 1 – which also serves to highlight the potential significance of these SUSY channels in the large m_{H^\pm} and intermediate $\tan\beta$ regions. In particular, we explore H^\pm decays into a chargino ($\tilde{\chi}_i^\pm$) and a neutralino ($\tilde{\chi}_j^0$); i.e., $H^\pm \rightarrow \tilde{\chi}_i^\pm \tilde{\chi}_j^0$, $i = 1$ or 2 and $j = 1, 2, 3$, or 4 . The lightest neutralino, $\tilde{\chi}_1^0$, is assumed to be the stable lightest SUSY particle (LSP). The decay width is given by [35]:

$$\begin{aligned} \Gamma(H^\pm \rightarrow \tilde{\chi}_i^\pm \tilde{\chi}_j^0) &= \left\{ g^2 \lambda^{1/2} [(F_L^2 + F_R^2)(m_{H^\pm}^2 - m_{\tilde{\chi}_i^\pm}^2 - m_{\tilde{\chi}_j^0}^2) - 4\epsilon F_L F_R m_{\tilde{\chi}_i^\pm} m_{\tilde{\chi}_j^0}] \right\} / \left\{ 16\pi m_{H^\pm}^3 \right\}, \quad (2) \end{aligned}$$

where F_L and F_R are as follows:

$$F_L = \cos\beta \left[N_{j4} V_{i1} + \sqrt{\frac{1}{2}} (N_{j2} + N_{j1} \tan\theta_W) V_{i2} \right],$$

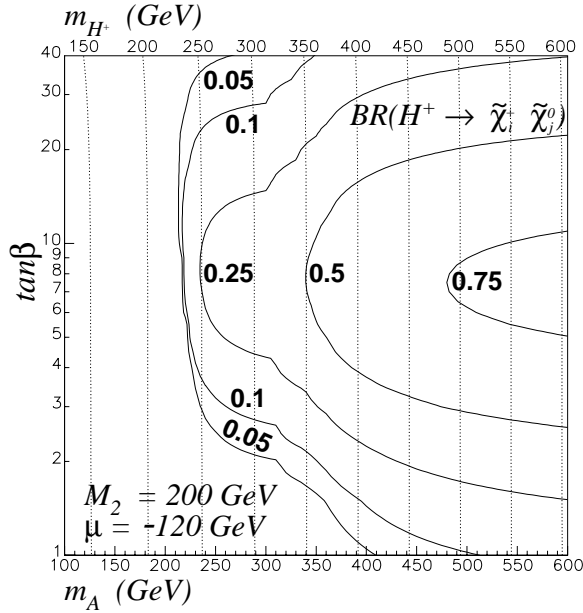


Fig. 1. BR’s of the MSSM charged Higgs boson into chargino–neutralino pairs (summing all such channels), in the $(m_A, \tan \beta)$ plane, with $M_2 = 200$ GeV and $\mu = -120$ GeV. One-loop formulæ as found in [34, 41] are used to relate m_{H^\pm} to m_A . Other MSSM input parameters are $m_{\tilde{q}}^{\text{soft}} = 1$ TeV, $A_t = 2$ TeV and $m_{\tilde{t}}^{\text{soft}} = 300$ GeV

$$F_R = \sin \beta \left[N_{j3} U_{i1} - \sqrt{\frac{1}{2}} (N_{j2} + N_{j1} \tan \theta_W) U_{i2} \right]. \quad (3)$$

(For the U , V and N matrices, we have followed the notation of [35].) Here, $m_{\tilde{\chi}_i^\pm}$ ($m_{\tilde{\chi}_j^0}$) are the masses corresponding to the $\tilde{\chi}_i^\pm$ ($\tilde{\chi}_j^0$) states and ϵ is the sign convention for the neutralino mass eigenstates. The dependence on the additional MSSM input parameters M_1 , M_2 , and μ enters from the gaugino/Higgsino mixing matrices via the U , V and N . M_1 and M_2 are the $U(1)_Y$ and $SU(2)_L$ gaugino masses, respectively, and μ is the Higgsino mass parameter. Grand unified theories (GUT’s) predict gaugino unification and $M_1 = (5/3) \tan^2 \theta_W M_2$, as will be assumed in all numerical calculations.

Branching ratios (BR’s) for the chargino–neutralino decay modes of the charged Higgs bosons are shown (along with the important SM decay BR’s) versus $\tan \beta$ in Fig. 2, choosing $M_2 = 200$ GeV and $\mu = -120$ GeV as in Fig. 1. While this point is favorable for chargino–neutralino decays, it did not result from an exhaustive search for the optimal choice. Three charged Higgs boson masses are examined ($m_{H^\pm} = 200, 300$, and 400 GeV). For $m_{H^\pm} = 200$ GeV, the only chargino–neutralino decay channel open is $\tilde{\chi}_1^\pm \tilde{\chi}_1^0$; whereas, for $m_{H^\pm} = 300$ GeV, the $\tilde{\chi}_1^\pm \tilde{\chi}_2^0$ and $\tilde{\chi}_1^\pm \tilde{\chi}_3^0$ channels are also accessible. In fact, in this latter case the BR for $H^\pm \rightarrow \tilde{\chi}_1^\pm \tilde{\chi}_2^0$ is larger than that for $H^\pm \rightarrow \tilde{\chi}_1^\pm \tilde{\chi}_1^0$ for $\tan \beta \gtrsim 2$. By the time m_{H^\pm} reaches 400 GeV, many chargino–neutralino decay channels have opened up and the situation becomes fairly complicated. Decays to the heaviest charginos and neutralinos may well

generate cascade decays rather than (predominantly) decaying directly to the LSP. This will introduce additional MSSM parameter space dependence as well as complicate the analysis. Further, as we shall see, for H^\pm masses much beyond this point, the lower top- H^\pm production rate robs us (after the necessary cuts) of any signal events in the multilepton channels we will be investigating. Therefore, there is considerable justification for concentrating upon the $H^\pm \rightarrow \tilde{\chi}_1^\pm \tilde{\chi}_1^0$, $\tilde{\chi}_1^\pm \tilde{\chi}_2^0$, $\tilde{\chi}_1^\pm \tilde{\chi}_3^0$ channels in this exploratory study.

Note from the $m_{H^\pm} = 400$ GeV plot in Fig. 2 that the sum of the various chargino–neutralino modes (which is represented by the “all SUSY” curve) does in fact dominate over the SM modes in the $\tan \beta$ range of interest. Note also that the combined BR’s to all the sleptons remains under (and usually well under) 2% even though (with $m_{\tilde{l}} \simeq 150$ GeV) such decay modes are open⁵. Charged Higgs boson decays into sfermions (squarks and sleptons), $H^- \rightarrow \tilde{q}\tilde{q}^*$, $\tilde{l}\tilde{l}^*$, are in fact heavily suppressed compared to the chargino–neutralino decay modes (by $\sim M_{W^\pm}/m_{H^\pm}$); and, typically, these BR’s do remain below the percent level.

In Fig. 2, the LEP2 bound on the mass of the chargino will exclude $\tan \beta$ values *above* a certain cut-off value. The exact value of this LEP2 bound⁶ depends slightly on the mass of the electron-flavor sneutrino. For a heavy $\tilde{\nu}_e$, the current LEP2 bound is $m_{\tilde{\chi}_1^\pm} \gtrsim 103.2$ GeV [36]. If $m_{\tilde{\nu}_e} \lesssim 200$ GeV, this bound is weakened by only a GeV or so; however, this small change is enough to shift the upper limit on allowable values for $\tan \beta$ from ~ 23 to ~ 39 . Also, as noted earlier, low values of $\tan \beta$ are excluded by LEP2 searches for a (neutral) Higgs boson. For this particular set of MSSM input parameters, we derive bounds of roughly $\tan \beta > 2.8, 2.4, 2.2$ (3.5, 2.9, 2.8) for $m_{H^\pm} = 200, 300, 400$ GeV based on the current (potential) LEP SM Higgs boson mass bounds given in the first (second) paper of [14]. Therefore, $3 < \tan \beta < 10$, the region where charged Higgs boson signatures from SM decays are virtually absent, and thus the region of primary interest to us in studying chargino–neutralino decay modes, is not excluded.

In this work, to avoid the enormous QCD background, only leptonic decays of the SUSY particles (sparticles) involved are considered⁷. Two specific signal types are analyzed: events containing either one or three hard leptons⁸ accompanied by missing transverse momentum, p_T^{miss} , and a reconstructed top (meaning a t - or \bar{t} -quark). The top

⁵ Exceptions to this general rule are found if the stau masses are lowered to the edge of the LEP2 excluded region ($m_{\tilde{\tau}_1} \sim 90$ GeV) and $m_{H^\pm} \lesssim 200$ GeV – see Borzumati and Djouadi in [30]

⁶ This does drop considerably if the chargino becomes near degenerate with the LSP; however, nowhere in the regions of parameter space we will investigate does this occur

⁷ Similar decays of neutral MSSM Higgs bosons were studied in [3, 37]

⁸ Hereafter, “leptons” will refer to electrons and muons in general and irrespective of sign; taus and neutrinos are not included

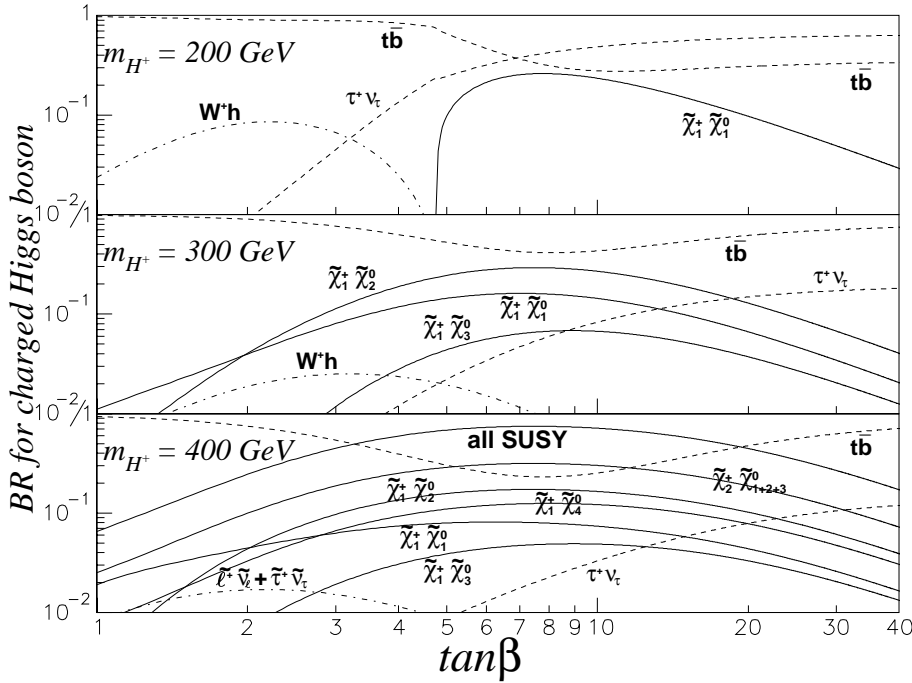


Fig. 2. BR's of the MSSM charged Higgs boson as a function of $\tan\beta$ for $m_{H^\pm} = 200, 300, \text{ and } 400$ GeV, again with $M_2 = 200$ GeV and $\mu = -120$ GeV. Other MSSM input parameters are also as in Fig. 1, except that here $m_{\tilde{\ell}}^{\text{soft}} = 150$ GeV

resonance is identified through the invariant mass of the three (at least at the parton level) jets resulting from its hadronic decay. (Here, we consider the rate for mis-identifying tops as very low and disregard any backgrounds that could arise from such mis-identification.) Tops decaying leptonically into a b -jet along with a charged lepton and a neutrino are not deemed to be part of the signal processes, but do play a rôle in potentially serious backgrounds and are included in all simulations (as are hadronically decaying charginos and neutralinos). The leptons result from the following three-body chargino and neutralino decays:

$$\tilde{\chi}_1^\pm \rightarrow \tilde{\chi}_1^0 \ell^\pm \tilde{\nu}_\ell^{(\pm)} \quad \text{and} \quad \tilde{\chi}_j^0 \rightarrow \tilde{\chi}_1^0 \ell^+ \ell^- \quad (j = 2, 3). \quad (4)$$

Note that the charginos and neutralinos decay directly to the LSP. Appropriate BR's for these decays are incorporated if necessary, but these are usually the only available decay modes. If the only virtual intermediate particles involved in these decays are the W^\pm and the Z^0 , then the leptonic BR's are the well-known leptonic BR's of the intermediate vector bosons (0.212 and 0.067, respectively). However, if sleptons are relatively light, they can also mediate these decays and significantly enhance the leptonic BR's [38] (especially those of the neutralinos), and thus also the rates for our prospective signals. Such light sleptons (with $m_{\tilde{\ell}}^{\text{soft}} \sim 150$ GeV) are not excluded experimentally and would not be out of place in the light MSSM sparticle spectrum under consideration.

In choosing the amount of missing transverse momentum required by the cuts, some knowledge of the chargino and neutralino mass spectrum is presumed to be available from independent measurements [39]. However, the charged Higgs boson mass is treated as a completely unknown parameter. Furthermore, due to the multiple particles leaving the detector unobserved, reconstruction of the

Higgs boson and sparticle masses involved in the signal decays is not possible. Rather we here content ourselves with looking for excesses in the specified modes above the SM expectations.

The analysis presented here is confined to the parton level only⁹: jets are identified with the partons from which they originate and jet selection criteria are applied directly to the partons. Typical detector resolutions (and range limitations) are included: the transverse momenta of all visible particles in the final state have been smeared according to a Gaussian distribution, with $(\sigma(p_T)/p_T)^2 = (0.6/p_T^{1/2})^2 + (0.04)^2$ for all jets and $(\sigma(p_T)/p_T)^2 = (0.12/p_T^{1/2})^2 + (0.01)^2$ for the leptons. The missing transverse momentum has been evaluated from the vector sum of the jet and lepton transverse momenta after resolution smearing. For reference, the CTEQ4L [43] structure function set is used, with the factorization scale set to $Q = m_t + m_{H^\pm}$ for the Higgs boson processes and $Q = m_t$ for all others. Aside from using running quark masses and loop-corrected Higgs boson masses, other higher order corrections to the tree level top- H^\pm production [44] and hadronic $H^\pm \rightarrow t\bar{b}$ decay [45] (which competes with our preferred SUSY decay modes) are not taken into account. The literature indicates that these corrections will not change the results much, though with small signals they should be kept in mind.

Following values given in [46], we assume a single b -tagging efficiency of $\epsilon_b = 0.5$ and a mis-tagging rate of $\epsilon_{\text{mis}} = 0.02$ (though we note the latter value may be too low since the study in [46] did not include c -quarks). How-

⁹ Although the signal processes have already been incorporated into the event generators HERWIG [40] and ISAJET [41], the incorporation of several important background processes (see below) is still in progress [42]

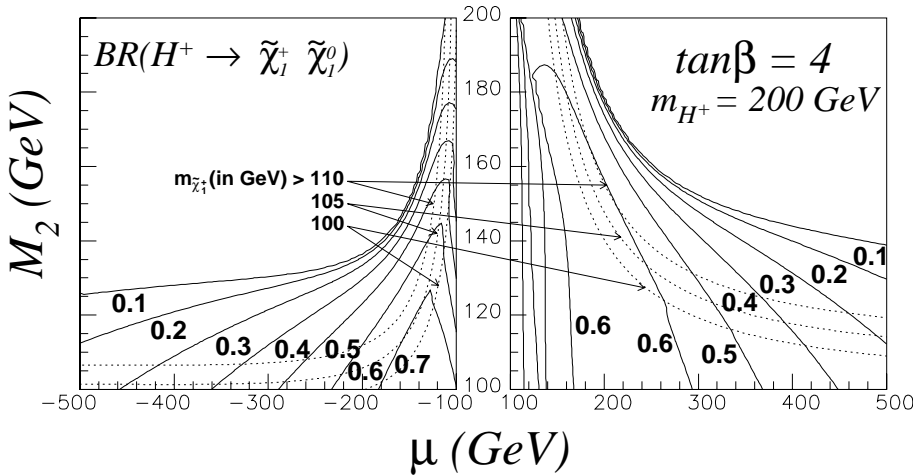


Fig. 3. $BR(H^+ \rightarrow \tilde{\chi}_1^+ \tilde{\chi}_1^0)$ in the (μ, M_2) plane for $\tan\beta = 4$ and $m_{H^\pm} = 200$ GeV. Other MSSM input parameters are as in Fig. 1. The dotted lines for $m_{\tilde{\chi}_1^\pm}$ indicate the reach of LEP2. As expected, setting $m_{\tilde{\ell}}^{\text{soft}} = 150$ GeV or $m_{\tilde{\ell}}^{\text{soft}} = 300$ GeV does not affect the results

ever, the \bar{b} -quark manifest in $gg \rightarrow \bar{b}tH^-$ is often expected to be soft and/or near the beam pipe. Thus, $\epsilon_b = 0.5$ is probably a serious over-estimation in this case. It is inappropriate to graft a serious b -tagging study onto this parton level analysis. A more thorough treatment will be presented in the upcoming event generator analysis [42]. As a simple approximation we adopt an on–off switch: if a b -jet (recall this is equivalent to a bottom quark) has a p_T above a certain specified value and an $|\eta|$ below another specified value, we assign a b -tagging efficiency of $\epsilon_b = 0.5$ to it; otherwise, we set $\epsilon_b = 0$ for that soft and/or too close to the beam pipe b -jet. Those b -jets stemming from top decays are expected to almost always pass this test, so we assume $\epsilon_b = 0.5$ for all such b -jets. Now, fortuitously, it so happens that, for the particular case of one versus two b -jets and $\epsilon_b = 0.5$, it does not matter how often there is one b -jet versus how often there are two b -jets fulfilling such criteria, since $\epsilon_b = 2\epsilon_b(1 - \epsilon_b) = 0.5$, and so the overall b -tagging efficiency for the event will remain 1/2. This is the case for the signals we are searching for as well as for all the backgrounds we will discuss.

We require one b -tagged jet in each event. This in fact reduces both the event rates *and* the signal to background ratios for the backgrounds we will consider explicitly. However, it also aids in triggering and the suppression of incidental QCD backgrounds which we do not attempt to calculate. In addition, we do veto events with more than one b -tagged jet. This does help in background reduction for all the backgrounds we consider as well as eliminating other bottom-rich event-types (such as $g\bar{b} \rightarrow t\bar{t}\bar{b}$, $g\bar{b} \rightarrow t\bar{t}\bar{b}$, $gg \rightarrow t\bar{t}\bar{b}\bar{b}$, etc.). We do not identify individual b -quarks as tagged or untagged, rather we multiply the event by a factor consistent with the values given above. Again, a more technical treatment is inconsistent with this parton level analysis and will come with the event generator studies.

1 The one-lepton signature: $\ell^\pm + p_T^{\text{miss}} + t$

If the charged Higgs boson is just above the top threshold, $m_{H^\pm} \simeq 200$ GeV, then it is quite likely that the only chargino–neutralino decay channel open will be $H^- \rightarrow$

$\tilde{\chi}_1^- \tilde{\chi}_1^0$, as is the case in Fig. 2. Schematically, the one lepton plus top signal would result from the reaction chain

$$gg \rightarrow \bar{b}tH^-, \quad t \rightarrow bq\bar{q}', \quad H^- \rightarrow \tilde{\chi}_1^- \tilde{\chi}_1^0, \quad \tilde{\chi}_1^- \rightarrow \tilde{\chi}_1^0 \ell^- \bar{\nu}_\ell, \quad (5)$$

($\ell = e, \mu$ and $q = d, u, s, c$). The hard lepton is derived from the decay of the chargino. The leptonic BR of the chargino is generally not as strongly affected by a light slepton as are those of the non-LSP neutralinos, though modest enhancement over the expectations from W^\pm -mediated decays are possible.

Figure 3 gives contour plots for $BR(H^\pm \rightarrow \tilde{\chi}_1^\pm \tilde{\chi}_1^0)$ with $m_{H^\pm} = 200$ GeV, $\tan\beta = 4$, and varying M_2 and μ – as noted earlier, these are the main other MSSM parameters to which the chargino and neutralino properties are sensitive. The region of parameter space excluded by the LEP2 bound on the chargino mass is indicated by the dotted curves which are, from bottom to top, contours for $m_{\tilde{\chi}_1^\pm} = 100, 105$, and 110 GeV. Note that the sensitivity to the exact bound here is much less than that of the $\tan\beta$ variable at the upper end of its range (see discussion of Fig. 2). BR’s for the desired charged Higgs boson decay channel in excess of 60% are possible in unexcluded MSSM parameter space even with this relatively low charged Higgs boson mass. Guided by the study of this BR, we have selected the following point in the MSSM parameter space for detailed simulations of the phenomenology of the one-lepton signature:

$$M_2 = 115 \text{ GeV}, \quad \mu = -200 \text{ GeV}, \quad \tan\beta = 4, \\ m_{H^\pm} = 200 \text{ GeV}. \quad (6)$$

At this point, the relevant masses and BR’s are

$$m_{\tilde{\chi}_{1,2}^\pm} = 112.61, 231.73 \text{ GeV}, \\ m_{\tilde{\chi}_{1-4}^0} = 59.86, 111.16, 219.43, 221.63 \text{ GeV}, \\ BR(H^- \rightarrow \tilde{\chi}_1^- \tilde{\chi}_1^0) = 0.56, \quad BR(H^- \rightarrow b\bar{t}) = 0.36, \\ BR(\tilde{\chi}_1^- \rightarrow \tilde{\chi}_1^0 \ell^- \bar{\nu}_\ell) = 0.28 \quad (\text{for } m_{\tilde{\ell}}^{\text{soft}} = 150 \text{ GeV}). \quad (7)$$

SM backgrounds to such events come from top pair production and single top production:

$$gg, q\bar{q} \rightarrow t\bar{t}, \quad t \rightarrow bq\bar{q}', \quad \bar{t} \rightarrow \bar{b}\ell^- \bar{\nu}_\ell, \quad (8)$$

$$gg, q\bar{q} \rightarrow t\bar{b}W^-, \quad t \rightarrow bq\bar{q}', \quad W^- \rightarrow \ell^- \bar{\nu}_\ell, \quad (9)$$

where the initial $\bar{b}W^-$ pair in (9) does not come from an on-shell top decay. At the LHC, approximately 0.1 billion $t\bar{t}$ events will be produced for every 100 fb^{-1} of integrated luminosity; whereas the corresponding number of top- H^\pm events is only several thousand – note that (9) is suppressed relative to (8) by $\sim \alpha_{\text{em}}$, meaning that rates for both backgrounds are larger than that of the would-be signal. Finally, the bottom–top decay of the charged Higgs boson may yet have an appreciable BR even when chargino–neutralino decay modes are very important. Such “ $H^- \rightarrow b\bar{t}$ ” events; i.e.,

$$gg \rightarrow \bar{b}tH^-, \quad t \rightarrow bq\bar{q}', \quad H^- \rightarrow b\bar{t}, \quad \bar{t} \rightarrow \bar{b}\ell^- \bar{\nu}_\ell$$

or

$$gg \rightarrow \bar{b}tH^-, \quad t \rightarrow b\ell^+ \nu_\ell, \quad H^- \rightarrow b\bar{t}, \quad \bar{t} \rightarrow \bar{b}q\bar{q}', \quad (10)$$

might also pass our signal cuts, though these are not designed to optimize the selection of $H^- \rightarrow b\bar{t}$ events which, for instance, have four b -jets manifest in the decay chains of (10), whereas only one tagged b -jet is permitted by our selection criteria. To cut out additional QCD backgrounds, such as the radiation of hard gluons from the afore-mentioned SM backgrounds (or MSSM gluino pair production followed by cascade decays), we will put a 4-jet cap¹⁰ on the number of jets we allow in any event. Adding the four b -jets above and two distinct (neglecting the rare case of jet mis-identification) untagged jets we will require to reconstruct a hadronically decaying W^\pm yields six jets, meaning most $H^- \rightarrow b\bar{t}$ events will also be lost to the 4-jet cut¹¹. Combined with the compulsory single tagged b -jet, this also implies that the surviving $H^- \rightarrow b\bar{t}$ events will have at least one and at most two b -jets passing our on–off switch criteria, and so the b -tagging efficiency factor for these surviving events will again be 1/2.

In our simulation, we have adopted the following acceptance and selection cuts:

(1) Jets and leptons are retained if they satisfy the following requirements: $p_{\text{T}}^{\ell,j} > 25 \text{ GeV}$, $|\eta_{\ell,j}| < 2$ and $\Delta R_{\ell,j/j,j}$

¹⁰ Of course, the jet number in an event can be affected, for example, by the merging of showers from different initial partons or hadrons lying too close to the beam pipe. A full event generator analysis should yield a more accurate estimate of the fraction of the time an expected jet is not seen than the present parton level analysis; so herein we will neglect such additional backgrounds

¹¹ Because of this, associated production, $gg, q\bar{q} \rightarrow W^+H^-$, with the W^+ providing the hard lepton and the top coming from $H^- \rightarrow b\bar{t}$, might be a mimic of comparable size to (5), our designated reaction chain, (even though the $W^\pm H^\mp$ production cross-section at this MSSM point is down by roughly an order of magnitude from top- H^\pm production) if a higher fraction of such events survive the cuts. However, since we will show explicitly that the reaction chains in (10) have a negligible effect, it is clear that this alternative reaction (or the even more suppressed charged Higgs pair production reaction chains) will also be unimportant

$= (\Delta\eta_{\ell,j/j,j}^2 + \Delta\phi_{\ell,j/j,j}^2)^{1/2} > 0.4$, where j represents both b -tagged and untagged jets. To pass this first cut, an event must have one and only one lepton that satisfies the above criteria and no more than four jets (irrespective of whether or not the jets are b -tagged) fulfilling the requirements.

(2) We require that $p_{\text{T}}^{\text{miss}} > 80 \text{ GeV}$.

(3) We demand that two untagged jets reproduce an invariant mass around M_{W^\pm} : $|M_{q\bar{q}'} - M_{W^\pm}| < 10 \text{ GeV}$. Therefore, to take into account the possibility of mistagging a jet as a b -jet, we will multiply the b -tagging factor to be applied at the end of the series of cuts by $(1 - 2\epsilon_{\text{mis}} + \epsilon_{\text{mis}}^2) = 0.96$.

(4) We combine these two light-quark-jets with a b -jet and demand that at least one such resulting 3-jet invariant mass be in the vicinity of m_t : $|M_{bq\bar{q}'} - m_t| < 25 \text{ GeV}$.

(5) Recognizing the difference in the number and type of particles leaving the detector undetected in the signal events (which have two LSP’s as well as neutrinos) and background events (which have only neutrinos – no LSP’s), we construct a variable to exploit this distinction, demanding that $(|p_{\text{T}}^{\text{miss}} - p_{\text{T}}^\ell|)/(|p_{\text{T}}^{\text{miss}} + p_{\text{T}}^\ell|) > 0.2$.

(6) Finally, we apply a veto on a leptonically decaying t - or \bar{t} -quark. If more than three jets (that is, jets in addition to the three jets already assigned to a hadronically decaying top in (3) and (4)) are present, then an invariant mass denoted by $M_{b\ell\nu_\ell}$ is formed from each extraneous jet’s four-momentum and those of the hard lepton and the missing momentum. The missing momentum is assumed to be solely due to a massless neutrino whose longitudinal momentum is reconstructed following the technique outlined in the first paper of [31]. This assignment is quite reasonable for SM double- and single-top events¹², so that the former can be eliminated with a cut of $|M_{b\ell\nu_\ell} - m_t| > 25 \text{ GeV}$. The assignment is of course not at all reasonable for decays of the charged Higgs boson, and simulations confirm that a far smaller fraction of these events are lost in comparison to the percentage of single- and double-top events weeded out.

Results for this series of cuts are given in Table 1. With an integrated luminosity of 100 fb^{-1} , about 265 signal events per year of run time survive. However, approximately 50,000 background events also survive. Even if one considers more favorable points in the MSSM parameter space, it is very difficult to enhance the signal cross-section significantly. Thus, if this one-lepton channel is to be useful in searching for charged Higgs boson at the LHC, far better cuts than those designed here will need to be devised.

2 The three-lepton signature:

$$\ell^\pm \ell^- \ell^+ + p_{\text{T}}^{\text{miss}} + t$$

For larger charged Higgs boson masses, other chargino–neutralino decay modes besides $H^- \rightarrow \tilde{\chi}_1^- \tilde{\chi}_1^0$ may well be

¹² Since neutrinos that may be produced in decays of B -mesons or further on down the decay chains inside the tagged and untagged b -jets are generally fairly soft

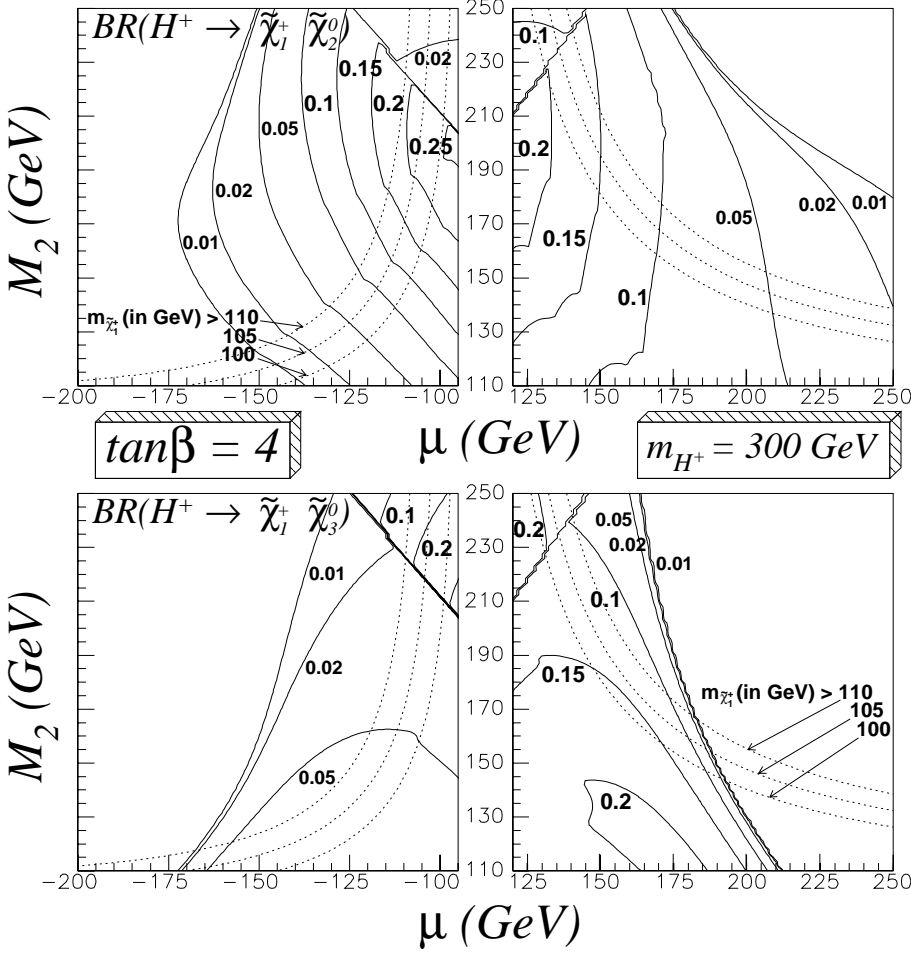


Fig. 4. $BR(H^+ \rightarrow \tilde{\chi}_1^+ \tilde{\chi}_2^0)$ (top) and $BR(H^+ \rightarrow \tilde{\chi}_1^+ \tilde{\chi}_3^0)$ (bottom) in the (μ, M_2) plane for $\tan\beta = 4$ and $m_{H^\pm} = 300$ GeV. Other MSSM input parameters are as in Fig. 1, except that $m_{\tilde{\ell}}^{\text{soft}} = 150$ GeV. The dotted lines for $m_{\tilde{\chi}_1^\pm}$ indicate the reach of LEP2

Table 1. Production and decay rates (in picobarns) for one-lepton signal and backgrounds, after the implementation of successive cuts. Rates already include the Higgs boson decay BR’s, whereas the common b -tagging \times mis-tagging factor of $(1/2) \times 0.96$ is not included. Also omitted are the BR for one top to decay hadronically (0.699) and the leptonic BR’s, 0.212 for the top decays and $BR(\tilde{\chi}_1^- \rightarrow \tilde{\chi}_1^0 \ell^- \bar{\nu}_\ell)$ for the signal, as well as the consequent combinatorial factor of 2

	$t\bar{t}$	$t\bar{b}W^-$	$H^- \rightarrow b\bar{t}$	$H^- \rightarrow \tilde{\chi}_1^- \tilde{\chi}_1^0$
No cuts	550.	71.	.20	.30
1 lepton with $p_T^\ell > 25$ GeV, $ \eta_\ell < 2, \Delta R_{\ell,j} > 0.4$	353.	36.	.15	.120
≤ 4 jets with $p_T^j > 25$ GeV, $ \eta_j < 2, \Delta R_{j,j} > 0.4$	153.	16.	.033	.042
$p_T^{\text{miss}} > 80$ GeV	28.	3.53	.0049	.025
$ M_{q\bar{q}'} - M_{W^\pm} < 10$ GeV	27.	3.38	.0040	.019
$ M_{b\bar{q}\bar{q}'} - m_t < 25$ GeV	25.	2.93	.0037	.018
$\frac{ p_T^{\text{miss}} - p_T^\ell }{ p_T^{\text{miss}} + p_T^\ell } > 0.2$	18.	2.65	.0029	.017
$ M_{b\bar{\ell}\nu_\ell} - m_t > 25$ GeV	1.99	1.49	.0005	.014

open and have sizable BR’s (as shown in Fig. 2). The heavier neutralinos may then decay leptonically, see (4), and, together with the chargino, produce three hard leptons

(as first discussed in [34]). Recall that in our notation “ ℓ ” stands for either electrons or muons. For the signal, two leptons with opposite signs must be of the same flavor; the third lepton may also be of the same flavor or of the other flavor. The expected reaction chain for the signal is

$$\begin{aligned}
gg &\rightarrow \bar{b}tH^-, \quad t \rightarrow bq\bar{q}', \quad H^- \rightarrow \tilde{\chi}_1^- \tilde{\chi}_{2,3}^0, \\
\tilde{\chi}_1^- &\rightarrow \tilde{\chi}_1^0 \ell^- \bar{\nu}_\ell, \quad \tilde{\chi}_{2,3}^0 \rightarrow \tilde{\chi}_1^0 \ell^- \ell^+.
\end{aligned}
\tag{11}$$

Figure 4 gives contour plots for $BR(H^\pm \rightarrow \tilde{\chi}_1^\pm \tilde{\chi}_2^0)$ (top) and $BR(H^\pm \rightarrow \tilde{\chi}_1^\pm \tilde{\chi}_3^0)$ (bottom), with $m_{H^\pm} = 300$ GeV, $\tan\beta = 4$, and again varying M_2 and μ . Limits of the regions excluded by LEP2 are again marked by dotted lines. BR’s above 20% are found at viable points in the parameter space. (The diagonal discontinuities seen in the upper right corners of the $\mu < 0$ plots and the upper left corners of the $\mu > 0$ plots are due to a “level-crossing” where the masses of $\tilde{\chi}_2^0$ and $\tilde{\chi}_3^0$ become degenerate – thus the identities of these two neutralinos are effectively interchanged as one of these diagonal lines is crossed.) From the study of these BR’s the following point in the MSSM parameter space was chosen for the simulation study:

$$\begin{aligned}
M_2 &= 200 \text{ GeV}, \quad \mu = -120 \text{ GeV}, \quad \tan\beta = 4, \\
m_{H^\pm} &= 300 \text{ GeV}, \quad m_{\tilde{\ell}}^{\text{soft}} = 150 \text{ GeV}.
\end{aligned}
\tag{12}$$

At this point, relevant masses and BR’s are

$$\begin{aligned}
m_{\tilde{\chi}_{1,2}^\pm} &= 116.85, 231.48 \text{ GeV}, \\
m_{\tilde{\chi}_{1-4}^0} &= 87.93, 122.01, 140.29, 230.76 \text{ GeV}, \\
\text{BR}(H^- \rightarrow \tilde{\chi}_1^- \tilde{\chi}_{2(3)}^0) &= 0.18(0.03), \\
\text{BR}(H^- \rightarrow b\bar{t}) &= 0.63, \\
\text{BR}(\tilde{\chi}_{2(3)}^0 \rightarrow \tilde{\chi}_1^0 \ell^+ \ell^-) &= 0.33(0.02), \\
\text{BR}(\tilde{\chi}_1^- \rightarrow \tilde{\chi}_1^0 \ell^- \bar{\nu}_\ell) &= 0.24. \tag{13}
\end{aligned}$$

Additional key variables to be aware of are $m_{\tilde{\chi}_1^-} - m_{\tilde{\chi}_1^0}$ and $m_{\tilde{\chi}_{2,3}^0} - m_{\tilde{\chi}_1^0}$. These are not so large here and this softens both the lepton spectra (the leptons coming from chargino and neutralino decays have on average lower transverse momenta than those coming from gauge boson decays) and that of p_T^{miss} . Another point worthy of mention is that the MSSM parameter point (12) gives $m_h = 105.5 \text{ GeV}$ if soft stop masses are set to 1 TeV and $A_t = 0$. With a projected LEP2 reach of $E_{\text{cm}} \simeq 208 \text{ GeV}$, this would yield a Higgsstrahlung cross-section that should be observable. However, if, for instance, A_t is raised to 2 TeV, then $m_h = 118.9 \text{ GeV}$ and on-shell Higgsstrahlung is kinematically forbidden. While soft SUSY-breaking parameters such as A_t can have a strong impact on m_h (as well as a possibly significant impact on the $b \rightarrow s\gamma$ rates, as will be discussed later), they have very little effect on m_{H^\pm} (as noted earlier). Thus some care must be taken that all relevant free parameters in the model are adequately explored so as to not neglect allowable MSSM parameter sets.

The dominant SM backgrounds are again those involving double- and single-top production and decay, this time accompanied by an additional lepton–antilepton pair (electrons or muons) produced in the “off-shell decay” of a neutral gauge boson ($V = \gamma/Z$)¹³:

$$\begin{aligned}
gg, q\bar{q} &\rightarrow t\bar{t}V^*, \quad t \rightarrow bq\bar{q}', \quad \bar{t} \rightarrow \bar{b}\ell^-\bar{\nu}_\ell, \\
V^* &\rightarrow \ell^-\ell^+, \tag{14}
\end{aligned}$$

and

$$\begin{aligned}
gg, q\bar{q} &\rightarrow t\bar{b}W^-V^*, \quad t \rightarrow bq\bar{q}', \quad W^- \rightarrow \ell^-\bar{\nu}_\ell, \\
V^* &\rightarrow \ell^-\ell^+. \tag{15}
\end{aligned}$$

The set of cuts applied is similar that employed for the one-lepton signal analysis:

(1) Jets and leptons are retained if they satisfy the following requirements: $p_T^\ell > 10 \text{ GeV}$, $p_T^j > 25 \text{ GeV}$, $|\eta_{\ell,j}| < 2$ and $\Delta R_{\ell,j/j,j} > 0.4$. The signal rate is sensitive to the p_T threshold for the leptons – lowering the threshold will enhance the signal survival rate more than that of the backgrounds. The value chosen here is reflective of the capabilities of the ATLAS detector [46]. As with the cuts for the one-lepton signal, for an event to pass this first cut it is compelled to have no more than four jets fulfilling the requirements. And in this case we of course demand that exactly three leptons also satisfy the criteria.

¹³ To assess the $t\bar{t}V^*$ background, the code originally developed in [47] was adapted to allow for an off-shell gauge boson

(2) We require that $p_T^{\text{miss}} > 25 \text{ GeV}$.

(3) As before, we impose $|M_{q\bar{q}'} - M_{W^\pm}| < 10 \text{ GeV}$.

(4) We also again impose $|M_{bq\bar{q}'} - m_t| < 25 \text{ GeV}$.

(5) Given the rather low missing momenta involved in both signal and backgrounds, we find that the variable $(|p_T^{\text{miss}} - p_T^\ell|)/(|p_T^{\text{miss}} + p_T^\ell|)$ used in the one-lepton analysis is no longer a suitable discriminant and do not include it in the cuts.

(6) Lastly, we apply a Z^0 veto, $|M_{\ell-\ell^+} - M_Z| > 10 \text{ GeV}$. This is to eliminate the SM backgrounds where the gauge boson is on- or nearly on-shell. Note that, for the signal, $m_{\tilde{\chi}_{2,3}^0} - m_{\tilde{\chi}_1^0} \ll M_Z$, and thus few signal events are lost here.

Results for this series of cuts are given in Table 2. Unlike in the case of the one-lepton signature, after cuts the three-lepton signal rate can be made competitive with the background rates. However, the total number of signal events is low. If one multiplies the final row of numbers of Table 2 by the b -tagging \times mis-tagging factor of $(1/2) \times 0.96$ and by the leptonic W^\pm and Z^0 BR’s (for first two columns) or the leptonic branching ratios from (13) (for the last two columns), one finds for one year’s running (100 fb^{-1}) the ratio signal events : background events = 7 : 20. Note that the enhanced leptonic BR of $\tilde{\chi}_2^0$ due to the light slepton intermediate state is very significant.

A more stringent cut can be applied on the invariant mass of the opposite sign lepton pair if we take advantage of the fact that $M_{\ell-\ell^+} < m_{\tilde{\chi}_{2,3}^0} - m_{\tilde{\chi}_1^0} < M_Z$. This entails the possession of some information about the masses of the lowest-lying sparticle states. As noted earlier, it is quite likely that such information will be available to those analyzing the real experimental data in search of a signal for the charged Higgs boson. (Note that it should also be possible to tune the $M_{\ell-\ell^+}$ limit to help optimize any observed signal even with incomplete information about the sparticle masses.) Seeing that the $\chi_1^0\chi_3^0$ contribution is not very important, we could impose the cut $M_{\ell-\ell^+} < m_{\tilde{\chi}_2^0} - m_{\tilde{\chi}_1^0}$, with the inclusion of which one finds for one year’s running the ratio signal events : background events = 5 : 5. Note that with the parameter set (12) and the consequent sparticle mass spectrum (13), cut (6) of Table 2 will be completely subsumed by this new cut. While this should be the case in general, it is safer to separately apply cut (6) and this new cut since the choice of the former is not parameter space dependent and the cut-off for the latter might rise above $M_Z - 10 \text{ GeV}$ in exceptional cases.

Another additional cut which has some dependence on the mass spectrum of the charginos and neutralinos can be applied by defining $M_T(3\ell) \equiv (2p_T^{3\ell} p_T^{\text{miss}} (1 - \cos \Delta\phi))^{1/2}$, where $p_T^{3\ell}$ is the transverse momentum of the three-lepton system and $\Delta\phi$ is the azimuthal separation between $p_T^{3\ell}$ and p_T^{miss} . Figure 5 illustrates how well this variable distinguishes our signal from the backgrounds. For the former, the $M_T(3\ell)$ distribution dies at $m_{H^\pm} - 2m_{\tilde{\chi}_1^0}$, which is $\approx 123 \text{ GeV}$ for the point (12), whereas, for the latter, it can stretch far beyond this value. Demanding $M_T(3\ell) < 100 \text{ GeV}$ yields the ratio signal events: background events = 7:9 (5:2), if applied on top of the cuts in Table 2 (or

Table 2. Production and decay rates (in femtobarns) for three-lepton signal and backgrounds, after the implementation of successive cuts. Rates already include the Higgs boson decay BR’s, whereas a common hadronic BR for the decaying top (0.699) and a common b -tagging \times mis-tagging factor of $(1/2) \times 0.96$ have been omitted. The SM backgrounds should also be multiplied by $2 \times 0.212 \times 0.066$ (accounting for the W^\pm and Z^0 leptonic BR’s), while the signal rates should be multiplied by $2 \times \text{BR}(\tilde{\chi}_1^- \rightarrow \tilde{\chi}_1^0 \ell^- \bar{\nu}_\ell) \times \text{BR}(\tilde{\chi}_{2(3)}^0 \rightarrow \tilde{\chi}_1^0 \ell^- \ell^+)$. The $t\bar{t}V^*$ and $t\bar{b}W^-V^*$ cross-sections ($V = \gamma, Z$) are expressible in terms of the Z^0 decay rates since, at the end of the series of cuts, the $Z^0 \rightarrow \ell^- \ell^+$ contribution is numerically dominant over the one from $\gamma^* \rightarrow \ell^- \ell^+$. Also note that, since m_ℓ is set to zero, a hard cut of $M_{\ell-\ell^+} > 10$ GeV is necessary to avoid the $\gamma^* \rightarrow \ell^- \ell^+$ singularity – this is included in the “No cuts” rates for $t\bar{b}W^-V^*$ and $t\bar{t}V^*$

	$t\bar{t}V^*$	$t\bar{b}W^-V^*$	$H^- \rightarrow \tilde{\chi}_1^- \tilde{\chi}_2^0$	$H^- \rightarrow \tilde{\chi}_1^- \tilde{\chi}_3^0$
No cuts	698.	111.	43.	7.0
3 leptons each with $p_T^\ell > 10$ GeV, $ \eta_\ell < 2, \Delta R(\ell, j) > 0.4$	317.	49.7	8.7	2.2
≤ 4 jets with $p_T^j > 25$ GeV, $ \eta_j < 2, \Delta R(j, j) > 0.4$	161.	30.3	1.75	.43
$p_T^{\text{miss}} > 25$ GeV	133.	21.1	1.67	.42
$ M_{q\bar{q}'} - M_{W^\pm} < 10$ GeV	126.	20.9	1.46	.39
$ M_{bq\bar{q}'} - m_\ell < 25$ GeV	110.	11.3	1.41	.33
$ M_{\ell-\ell^+} - M_Z > 10$ GeV	17.	5.03	1.38	.32

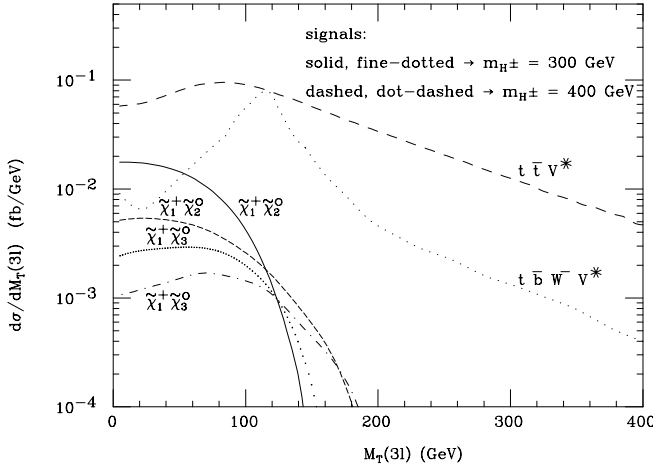


Fig. 5. Normalized differential distributions of the three-lepton system transverse mass, $M_T(3\ell)$ (as defined in the text) for $H^+ \rightarrow \tilde{\chi}_1^+ \tilde{\chi}_2^0$ (solid: $m_{H^\pm} = 300$ GeV; dashed: $m_{H^\pm} = 400$ GeV), $H^+ \rightarrow \tilde{\chi}_1^+ \tilde{\chi}_3^0$ (fine-dotted: $m_{H^\pm} = 300$ GeV; dot-dashed: $m_{H^\pm} = 400$ GeV), $t\bar{t}V^*$ (long-dashed), and $t\bar{b}W^-V^*$ (dotted). Here $M_2 = 200$ GeV, $\mu = -120$ GeV and $\tan\beta = 4$. Other MSSM input parameters are as in Fig. 1. Normalizations are as after the cuts in Table 2; i.e., the leptonic BR’s and the b -tagging \times mis-tagging efficiency are not included

in conjunction with strengthening the $|M_{\ell-\ell^+} - M_Z| > 10$ GeV cut in Table 2 to $M_{\ell-\ell^+} < m_{\tilde{\chi}_2^0} - m_{\tilde{\chi}_1^0}$.

Bolstered somewhat by this result, it is reasonable to consider still higher charged Higgs boson masses. Now competing factors come into play. On the one hand, the three-lepton chargino–neutralino decay channels remain

large – with $m_{H^\pm} = 400$ GeV and all other MSSM parameters the same as in point (12), one has $\text{BR}(H^- \rightarrow \tilde{\chi}_1^- \tilde{\chi}_2^0) = 0.14$ and $\text{BR}(H^- \rightarrow \tilde{\chi}_1^- \tilde{\chi}_3^0) = 0.03$ – and, on the positive side, the lepton spectrum becomes harder. On the other hand, the top– H^\pm production rate drops precipitously, by more than a factor of 2 when m_{H^\pm} is increased from 300 GeV to 400 GeV. Unfortunately the latter negative effect dominates: although a greater percentage of the signal events survive the cuts, one starts with a production cross-section that is just too small. Applying the same cuts as in Table 2 for $m_{H^\pm} = 400$ GeV yields 0.55 fb and 0.20 fb for the $H^- \rightarrow \tilde{\chi}_1^- \tilde{\chi}_2^0$ and $H^- \rightarrow \tilde{\chi}_1^- \tilde{\chi}_3^0$ channels, respectively. Adopting the same b -tagging efficiencies and leptonic BR’s as for the $m_{H^\pm} = 300$ GeV case now yields (for $m_{H^\pm} = 400$ GeV) the ratio signal events : background events = 3 : 20. In addition, the larger m_{H^\pm} means the extra $M_T(3\ell)$ cut must be weakened – requiring $M_T(3\ell) < 120$ GeV along with $|M_{\ell-\ell^+} - M_Z| > 10$ GeV leads to the ratio signal events : background events = 3 : 11. Also, since the $H^- \rightarrow \tilde{\chi}_1^- \tilde{\chi}_3^0$ decay modes accounts for more of the signal now, if the $M_{\ell-\ell^+} < m_{\tilde{\chi}_2^0} - m_{\tilde{\chi}_1^0}$ cut is implemented, more signal will be lost, while a weaker $M_{\ell-\ell^+} < m_{\tilde{\chi}_3^0} - m_{\tilde{\chi}_1^0}$ cut is much less effective at cutting away backgrounds. Thus, both the total three-lepton signal event rate and its statistical significance decline as m_{H^\pm} is raised from 300 GeV to 400 GeV. To this though must be added the caveat that, at $m_{H^\pm} = 400$ GeV, decay modes including either the heaviest chargino or the heaviest neutralino are significant (as seen from Fig. 2). We have neglected these, and so our results may be viewed as conservative. But it is nonetheless evident that $m_{H^\pm} = 400$ GeV is near the kinematical limit beyond which there is

too little top– H^\pm production cross-section at the LHC to exploit through the chargino–neutralino decay channels.

In contrast, for $m_{H^\pm} \lesssim 400$ GeV, $\tan\beta$ values up to ~ 10 can be scanned (for a significant portion of the possible values of the other MSSM input parameters) using the tripleton plus top signature from $H^\pm \rightarrow \tilde{\chi}_1^\pm \tilde{\chi}_{2,3}^0$ decays. In fact, over the range $3 \lesssim \tan\beta \lesssim 10$, as $\tan\beta$ gets larger, the enhancement (or suppression) of the Higgs decay rates is compensated by an opposite effect in the production rate. This is understandable since the BR's for $H^\pm \rightarrow \tilde{\chi}_i^\pm \tilde{\chi}_j^0$ strengthen as the $H^- \rightarrow b\bar{t}$ decay width weakens (as can be seen from an examination of Fig. 2), and the latter is proportional to the square of the same coupling (1) as the top– H^\pm production modes. Beyond $\tan\beta \approx 10$, the $\text{BR}(H^\pm \rightarrow \tilde{\chi}_i^\pm \tilde{\chi}_j^0)$'s start falling below the $\tan\beta = 4$ values simulated in the preceding numerical analyses. In fact, due to the strengthening of other alternative decay modes (such as $H^- \rightarrow \tau^- \bar{\nu}_\tau$), these BR's fall even quicker than the top– H^\pm production rate increases.

Since the event rate imposes a discovery limit ($\lesssim 400$ GeV) on the mass of the charged Higgs bosons, it is important to determine if all or part of the region of parameter space where the signal seems observable is excluded by constraints coming from $b \rightarrow s\gamma$ decays. At present however, we are unaware of any clean answer to this question. To circumvent the $b \rightarrow s\gamma$ constraint with such modest charged Higgs boson masses, there must be sufficient cancellation between the contributions from the top–charged Higgs boson loop and the chargino–stop loop (we assume contributions from gluino–squark loops [48] are negligible, though this need not always be true). Seeing that our signal stems from charged Higgs boson decays including a chargino (this prefers, among other things, lower values for $|\mu|$), it follows that the main freedom left to adjust the $b \rightarrow s\gamma$ rates lies in the stop sector¹⁴. The MSSM stop input parameters must be large enough to boost the light Higgs boson mass above the LEP2 bounds (for the sample point we have used for illustration, this would translate into stop masses in the ~ 400 – 600 GeV ballpark), yet low enough to ensure sufficient cancellation among the MSSM $b \rightarrow s\gamma$ diagrams (see [10], Fig. 19, for a rough idea). Studies addressing this have been done in the more restrictive mSUGRA scenario (see for example Goto and Okada [13]; note though that this is a leading order calculation, and that more recent next-to-leading order studies suggest there may be significant modifications to these results – see Ciuchini et al. and Bobeth et al. [13]), and point toward a severe curtailment of the range of open parameter space for our signal. However, in mSUGRA the stop parameters are related to those of the Higgs bosons and the Higgsinos. If a more general MSSM scenario is assumed,

¹⁴ Here we are operating under the assumption that inter-generational squark mixing is negligible, analogous to the case for the third generation of the CKM matrix. If squark mixings are made arbitrary, the $b \rightarrow s\gamma$ constraint can almost certainly be evaded; however, constraints from other flavor-changing neutral current processes need to be considered as well

these relationships will disappear, and the restriction from $b \rightarrow s\gamma$ may well be significantly relaxed.

One final issue to consider is the distinguishability of the charged Higgs bosons from the neutral H and A . Throughout much of the parameter space, these MSSM Higgs bosons all have very similar masses. Background to the charged Higgs boson signal could come from $gg, q\bar{q} \rightarrow t\bar{t}H, t\bar{t}A$ [2, 49] or $q\bar{q}' \rightarrow t\bar{b}H, t\bar{b}A$ production [50], where the neutral MSSM Higgs boson then decays into chargino or neutralino pairs. Fortunately, for the moderate $\tan\beta$ values we are interested in here, the $t\bar{t}H$ and $t\bar{t}A$ production rates at the LHC are about an order of magnitude lower than the top– H^\pm production rate. (See also the second paper of [32].)

In summary, chargino–neutralino decays of heavy (i.e., with $m_{H^\pm} \gtrsim m_t$) MSSM charged Higgs bosons have some potential to aid in the detection of such H^\pm scalars at the LHC, especially in the intermediate $\tan\beta$ region, $3 \lesssim \tan\beta \lesssim 10$, which is inaccessible via SM decays¹⁵. Among the possible chargino–neutralino combinations, the most promising are the $H^- \rightarrow \tilde{\chi}_1^- \tilde{\chi}_2^0, \tilde{\chi}_1^- \tilde{\chi}_3^0$ decays followed in turn by the decays $\tilde{\chi}_1^- \rightarrow \tilde{\chi}_1^0 \ell^- \bar{\nu}_\ell$ and $\tilde{\chi}_{2,3}^0 \rightarrow \tilde{\chi}_1^0 \ell^+ \ell^-$, yielding a three-lepton final state. (The decay $H^- \rightarrow \tilde{\chi}_1^- \tilde{\chi}_1^0$ leading to a one-lepton final state was also studied, but found to be overwhelmed by the SM backgrounds.) Since the charged Higgs boson is dominantly produced in association with a top quark, the main signature to look for is three hard, isolated leptons plus significant p_T^{miss} and a reconstructed top quark. Unfortunately, after the cuts utilized in this simulation, the surviving signal event rates are small – only around a handful of events per year. Furthermore, these rates are sensitive to several MSSM parameters, including M_2 , μ , and (via the leptonic BR's of $\tilde{\chi}_{2,3}^0$) $m_{\tilde{\ell}}^{\text{soft}}$. However, given the paucity of handles which can be used to study charged Higgs boson production at the LHC for intermediate $\tan\beta$ values, further investigation of even such weak signals in the more realistic environment of a full event generator, including parton shower effects and hadronization, would be clarifying and beneficial. Such a study is well underway (using the HERWIG [40] and ISAJET [41] event generators) and we plan to report the results from these studies in the near future [42].

Acknowledgements. MB is grateful to the U.S. National Science Foundation for support under grant INT-9804704 and also to the DESY theory group and the Physics Department of the Technion for warm hospitality during portions of this study. He also thanks P. Mercadante for very helpful correspondence. MG is thankful to D. Zeppenfeld for fruitful discussions and to the Theory Group at Saha Institute of Nuclear Physics for hospitality during the final phase of this work. SM is grateful to PPARC for financial support. He also thanks K.A. Assamagan and Y. Coadou for useful conversations. The authors thank F. Borzumati, M. Misiak and Y. Okada for helpful information

¹⁵ Chargino–neutralino decays could of course also hinder detection in other $\tan\beta$ regions by suppressing the BR's of SM decay modes that do yield signals. This also merits further attention

concerning $b \rightarrow s\gamma$. They also thank X. Tata and P. Zerwas for their careful reading of the manuscript and their sagacious suggestions.

References

1. J. Gunion, L. Orr, Phys. Rev. D **46**, 2052 (1992)
2. Z. Kunszt, F. Zwirner, Nucl. Phys. B **385**, 3 (1992)
3. H. Baer, M. Bisset, D. Dicus, C. Kao, X. Tata, Phys. Rev. D **47**, 1062 (1993)
4. D. Cavelli et al., preprint ATL-PHYS-96-074; G.L. Bayatian et al. (CMS Collaboration), Technical Design Report, CERN/LHCC 94-38, December 1994
5. J.F. Gunion, H.E. Haber, G.L. Kane, S. Dawson, The Higgs hunter guide (Addison-Wesley, Reading MA 1990), Erratum: University of California, Santa Cruz, preprint SCIPP-92-58, February 1993, hep-ph/9302272
6. Y. Okada, H. Yamaguchi, T. Yanagida, Prog. Theor. Phys. Lett. **85**, 1 (1991); H.E. Haber, R. Hemfling, Phys. Rev. Lett. **66**, 1815 (1991); J. Ellis, G. Ridolfi, F. Zwirner, Phys. Lett B **257**, 83 (1991); see A. Dedes et al., hep-ph/9912249 and references therein for current status and review
7. S. Heinemeyer, W. Hollik, G. Weiglein, Eur. Phys. J. C **9**, 343 (1999)
8. A. Brignole, J. Ellis, G. Ridolfi, F. Zwirner, Phys. Lett. B **271**, 123 (1991); A. Brignole, Phys. Lett. B **277**, 313 (1992); M.A. Díaz, H.E. Haber, Phys. Rev. D **45**, 4246 (1992)
9. M. Drees, E. Ma, P.N. Pandita, D.P. Roy, S.K. Vempati, Phys. Lett. B **433**, 346 (1998)
10. M. Misiak, S. Pokorski, J. Rosiek, in: Heavy Flavors II (World Scientific, Singapore 1990), edited by A.J. Buras, M. Lindner, pp. 795–828, hep-ph/9703442
11. P.H. Chankowski, S. Pokorski, in: Perspectives in supersymmetry (World Scientific, Singapore, 1997), edited by G.L. Kane, pp. 402–422, hep-ph/9707497
12. J. Erler, D.M. Pierce, Nucl. Phys. B **526**, 53 (1998)
13. S. Bertolini, F. Borzumati, A. Masiero, G. Ridolfi, Nucl. Phys. B **353**, 591 (1991); A.J. Buras, M. Misiak, M. Munz, S. Pokorski, Nucl. Phys. B **424**, 374 (1994); F.M. Borzumati, Z. Phys. C **63**, 291 (1994); P. Cho, M. Misiak, D. Wyler, Phys. Rev. D **54**, 3329 (1996); T. Goto, Y. Okada, Prog. Theor. Phys. Suppl. **123**, 213 (1996); M. Ciuchini, G. Degrassi, P. Gambino, G.F. Giudice, Nucl. Phys. B **534**, 3 (1998); F.M. Borzumati, C. Greub, Phys. Rev. D **58**, 074004 (1998); Phys. Rev. D **59**, 057501 (1999); hep-ph/9810240; M.A. Díaz, E. Torrente-Lujan, J.F.W. Valle, Nucl. Phys. B **551**, 78 (1999); C. Bobeth, M. Misiak, J. Urban, Nucl. Phys. B **567**, 153 (2000); for discussion of the current status of $b \rightarrow s\gamma$ calculations, see M. Misiak, hep-ph/0009033
14. P. Bock et al. (The LEP working group for Higgs boson searches), preprint CERN-EP-2000-055, April, 2000; A. Read, Status of searches for Higgs bosons at LEP with $s^{1/2} \leq 210$ GeV, LEPC 20.7.2000. Both can be found via the LEP Higgs Working Group web page, <http://lephiggs.web.cern.ch/LEPHIGGS/>
15. A. Sopczak, Z. Phys. C **65**, 449 (1995)
16. R.M. Godbole, D.P. Roy, Phys. Rev. D **43**, 3640 (1991); D.P. Roy, Phys. Lett. B **283**, 403 (1992); *ibid.* B **277**, 183 (1992); S. Raychaudhuri, D.P. Roy, Phys. Rev. D **52**, 1556 (1995); *ibid.* D **53**, 4902 (1996); see also [3]. For most recent Tevatron results, see T. Affolder et al. (CDF Collaboration), Phys. Rev. D **62**, 012004 (2000)
17. E. Ma, D.P. Roy, J. Wudka, Phys. Rev. Lett. **80**, 1162 (1998)
18. See, e.g.: M. Carena, J. Conway, H.E. Haber, J. Hobbs, Report of the Higgs Working Group, to appear in the Proceedings of the Tevatron Run II SUSY/Higgs Workshop, February–November 1998, Fermilab, Batavia, Illinois (unpublished)
19. K. Odagiri, private communication
20. K.A. Assamagan, A. Djouadi, M. Drees, M. Guchait, R. Kinnunen, J.L. Kneur, D.J. Miller, S. Moretti, K. Odagiri, D.P. Roy, contribution to the Workshop Physics at TeV Colliders, Les Houches, France, 8–18 June 1999, preprint PM/00-03, pp. 36–53, February 2000, hep-ph/0002258 (to appear in the proceedings)
21. J.F. Gunion, H.E. Haber, F.E. Paige, W.-K. Tung, S.S.D. Willenbrock, Nucl. Phys. B **294**, 621 (1987)
22. J.L. Diaz-Cruz, O.A. Sampayo, Phys. Rev. D **50**, 6820 (1994)
23. S. Moretti, K. Odagiri, Phys. Rev. D **55**, 5627 (1997); H.-J. He, C.P. Yuan, Phys. Rev. Lett. **83**, 28 (1999); C. Balazs, H.-J. He, C.P. Yuan, Phys. Rev. D **59**, 055016 (1999); *ibid.* D **60**, 114001 (1999)
24. A. Krause, T. Plehn, M. Spira, P.M. Zerwas, Nucl. Phys. B **519**, 85 (1998); Y. Jiang, W.-G. Ma, L. Han, M. Han, Z.-H. Yu, J. Phys. G **24**, 83 (1998); A.A. Barrientos Bendeziú, B.A. Kniehl, Nucl. Phys. B **568**, 305 (2000); O. Brein, W. Hollik, Eur. Phys. J. C **13**, 175 (2000)
25. D.A. Dicus, J.L. Hewett, C. Kao, T.G. Rizzo, Phys. Rev. D **40**, 787 (1989); A.A. Barrientos Bendeziú, B.A. Kniehl, Phys. Rev. D **59**, 015009 (1999); *ibid.* D **61**, 097701 (2000); *ibid.* D **63**, 015009 (2001); O. Brein, W. Hollik, S. Kanemura, KA-TP-14-2000, Aug. 2000, hep-ph/0008308
26. S. Moretti, K. Odagiri, Phys. Rev. D **59**, 055008 (1999); results for τ decays by S. Moretti not yet published
27. J.F. Gunion, Phys. Lett. B **322**, 125 (1994)
28. F. Borzumati, J.-L. Kneur, N. Polonsky, Phys. Rev. D **60**: 115011 (1999)
29. D. Dicus, T. Stelzer, Z. Sullivan, S. Willenbrock, Phys. Rev. D **59**, 094016 (1999)
30. S. Moretti, W.J. Stirling, Phys. Lett. B **347**, 291 (1995); *ibid.* B **366**, 451 (1996); A. Djouadi, J. Kalinowski, P.M. Zerwas, Z. Phys. C **70**, 435 (1996); A. Djouadi, P. Janot, J. Kalinowski, P.M. Zerwas Phys. Lett. B **376**, 220 (1996); F.M. Borzumati, A. Djouadi, hep-ph/9806301; see also [20, 34]
31. V. Barger, R.J.N. Phillips, D.P. Roy, Phys. Lett. B **324**, 236 (1994); S. Moretti, D.P. Roy, Phys. Lett B **470**, 209 (1999); D.J. Miller, S. Moretti, D.P. Roy, W.J. Stirling, Phys. Rev. D **61**, 055011 (2000); ATLAS simulation: K.A. Assamagan, preprint ATL-PHYS-99-013
32. M. Drees, M. Guchait, D.P. Roy, Phys. Lett. B **471**, 39 (1999); S. Moretti, Phys. Lett. B **481**, 49 (2000); ATLAS simulation: K.A. Assamagan, preprint ATL-PHYS-99-025
33. K. Odagiri, preprint RAL-TR-1999-012, February 1999, hep-ph/9901432; D.P. Roy, Phys. Lett. B **459**, 607 (1999); ATLAS simulation: K.A. Assamagan, Y. Coadou, preprint ATL-COM-PHYS-2000-017
34. M. Bisset, University of Hawaii at Manoa Ph.D. Dissertation, UH-511-813-94 (1994)

35. J.F. Gunion, H.E. Haber, Nucl. Phys. B **307**, 445 (1988);
ibid. B **272**, 1 (1986); Erratum, ibid. B **402**, 567 (1993)
36. See, e.g., LEP SUSY Working Group web page,
<http://www.cern.ch/LEPSUSY/>
37. H. Baer, M. Bisset, C. Kao, X. Tata, Phys. Rev. D **50**, 316
(1994)
38. H. Baer, X. Tata, Phys. Rev. D **47**, 2739 (1993)
39. G. Montarou, S. Muanza, preprint ATL-PHYS-97-099; G.
Bélanger, F. Boudjema, F. Donato, R. Godbole, S. Rosier-
Lees, Nucl. Phys. B **581**, 3 (2000)
40. G. Corcella, I.G. Knowles, G. Marchesini, S. Moretti,
K. Odagiri, P. Richardson, M.H. Seymour, B.R. Web-
ber, preprint Cavendish-HEP-99/03, CERN-TH/2000-
284, RAL-TR-2000-048, November 2000, hep-ph/0011363,
preprint Cavendish-HEP-99/17, December 1999, hep-
ph/9912396 (and references therein)
41. H. Baer, F.E. Paige, S.D. Protopopescu, X. Tata, preprint
BNL-HET-99-43, FSU-HEP-991218, UH-511-952-00, De-
cember 1999, hep-ph/0001086 (and references therein)
42. M. Bisset, M. Guchait, S. Moretti, in preparation
43. H.L. Lai, J. Huston, S. Kuhlmann, F. Olness, J. Owens,
D. Soper, W.K. Tung, H. Weerts, Phys. Rev. D **55**, 1280
(1997)
44. L.G. Jin, C.S. Li, R.J. Oakes, S.H. Zhu, Phys. Rev. D **62**,
053008 (2000); Eur. Phys. J. C **14**, 91 (2000)
45. A. Mendez, A. Pomarol, Phys. Lett. B **252**, 461 (1990);
ibid. B **265**, 177 (1991); C.S. Li, R.J. Oakes, Phys. Rev. D
43, 855 (1991); M. Drees, D.P. Roy, Phys. Lett. B **269**, 155
(1991); J.M. Yang, C.S. Li, B.Q. Hu, Phys. Rev. D **47**,
2872 (1993); A. Bartl, K. Hidaka, Y. Kizukuri, T. Kon,
W. Majerotto, Phys. Lett. B **315**, 360 (1993); A. Bartl,
H. Eberl, K. Hidaka, T. Kon, W. Majerotto, Y. Yamada,
Phys. Lett. B **378**, 167 (1996); A. Djouadi, P. Gambino,
Phys. Rev. D **51**, 218 (1995); Erratum, ibid. D **53**, 4111
(1996); A. Djouadi, M. Spira, P.M. Zerwas, Z. Phys. C **70**,
427 (1996); R.A. Jimenez, J. Sola, Phys. Lett. B **389**, 53
(1996); J.A. Coarasa, D. Garcia, J. Guasch, R.A. Jimenez,
J. Sola, Phys. Lett. B **425**, 329 (1998); corrections to the
 $H^\pm \rightarrow hW^\pm$ decay were studied in R. Santos, A. Barroso,
L. Brucher, Phys. Lett. B **391**, 429 (1997); Y.S. Yang, C.S.
Li, PKU-TH-2000-98, September 2000, hep-ph/0009346
46. W.W. Armstrong et al. (ATLAS Collaboration), Technical
Design Report, CERN/LHCC/94-43, December 1994
47. E. Maina, S. Moretti, Phys. Lett. B **286**, 370 (1992)
48. S. Bertolini, F. Borzumati, A. Masiero, Phys. Lett. B **192**,
437 (1987); F. Borzumati, C. Greub, T. Hurth, D. Wyler,
Phys. Rev. D **62**, 075005 (2000)
49. Z. Kunszt, S. Moretti, W.J. Stirling, Z. Phys. C **74**, 479
(1997); E. Richter-Was, M. Sapinski, Acta Phys. Pol. B
30, 1001 (1999)
50. W.J. Stirling, D.J. Summers, Phys. Lett. B **283**, 411
(1992); A. Ballestrero, E. Maina, Phys. Lett. B **299**, 312
(1993); G. Bordes, V. van Eijk, Phys. Lett. B **299**, 315
(1993)